

# Rare-Earth Clustering and Aluminum Codoping in Sol-Gel Silica: Investigation Using Europium(III) Fluorescence Spectroscopy

Michael J. Lochhead<sup>†</sup> and Kevin L. Bray<sup>\*</sup>

Department of Chemical Engineering and the Materials Science Program,  
University of Wisconsin, Madison 53706

Received October 25, 1994. Revised Manuscript Received January 9, 1995<sup>®</sup>

Eu<sup>3+</sup> fluorescence spectroscopy is used to investigate the clustering of rare-earth ions and the effectiveness of aluminum codoping in dispersing and isolating rare-earth ions in sol-gel silica monoliths. Fluorescence line-narrowing (FLN) studies are demonstrated as a useful tool in identifying clustered and isolated Eu<sup>3+</sup>. Clustered Eu<sup>3+</sup> is identified by the lack of a line-narrowing effect, which is attributed to energy transfer between adjacent Eu<sup>3+</sup> ions. Clustering is shown to be significant, even in transparent samples with Eu<sup>3+</sup> concentrations as low as 0.5 wt % Eu<sup>3+</sup>. Addition of Al<sup>3+</sup> as a codopant has a profound impact on the bonding and structure of Eu<sup>3+</sup> in silica. Significant fluorescence line narrowing is observed, which suggests that Al<sup>3+</sup> codoping is effective in dispersing and isolating Eu<sup>3+</sup> ions in the silica matrix. Fluorescence decay studies provide evidence of increased Eu<sup>3+</sup> hydroxylation in the Al<sup>3+</sup>-containing samples.

## Introduction

The incorporation of inorganic ions into silica gels and glasses is of interest for a variety of technological applications, including optical devices such as fiber amplifiers and solid-state lasers.<sup>1,2</sup> Of particular interest are rare-earth-ion-based systems.<sup>1</sup> The sol-gel process is a potentially attractive means of synthesizing these materials, since it offers a degree of control over the microstructure and composition of the host matrix and the opportunity to prepare new materials.<sup>3</sup> Significant research into the structural evolution of silica gels has been performed in the past 15 years.<sup>3</sup> A detailed understanding of the incorporation of dopant ions in these materials, however, is not well-established. Since the optical properties of doped silica systems depend intimately on the local structure and bonding of dopant cations, a detailed understanding of these factors is important from a device engineering perspective.

This paper focuses on silicon alkoxide-based, monolithic samples doped with Eu<sup>3+</sup>. Monolithic samples were selected because the structural evolution of undoped, monolithic silica has been studied in detail.<sup>3</sup> The introduction of dopant ions acts as a perturbation of this well-studied system. Eu<sup>3+</sup> was selected as a representative rare-earth ion because its unique fluorescence properties make it an outstanding probe of local structure.<sup>4</sup> Eu<sup>3+</sup> spectroscopy has previously been used to

characterize gelation and densification of silica gels.<sup>5-14</sup> A conclusion of this previous work was that as the densification temperature is increased, the Eu<sup>3+</sup> bonding environment approaches what is observed in traditional, melt-derived silicate glasses. While this conclusion is qualitatively correct, evidence is presented in this paper suggesting that Eu<sup>3+</sup> ions are significantly clustered in sol-gel silica even at low concentrations (<1 wt % Eu<sub>2</sub>O<sub>3</sub>). This observation is important in that dopant ion clustering generally has adverse effects on optical properties.

Several researchers have noted that codoping with Al<sup>3+</sup> is effective at dispersing rare earth ions in silica gel and silicate glass matrices.<sup>15-19</sup> A detailed interpretation of why and when rare earth-ion isolation occurs, however, has not been established.

(5) Levy, D.; Reinfeld, R.; Avnir, D. *Chem. Phys. Lett.* **1984**, *109*, 593.

(6) Lochhead, M. J.; Bray, K. L. *J. Non-Cryst. Solids* **1994**, *170*, 143.

(7) Lochhead, M. J.; Bray, K. L. In *Better Ceramics Through Chemistry VI*; Cheetham, A. K., Brinker, C. J., Mecartney, M. L., Sanchez, C., Eds.; Materials Research Society: Pittsburgh, 1994; p 745-750.

(8) Lochhead, M. J.; Bray, K. L. In *Sol-Gel Optics III*; Mackenzie, J. D., Ed.; *Proc. SPIE* **1994**, *2288*, 688.

(9) McDonagh, C.; Ennis, G.; Marron, P.; O'Kelly, B.; Tang, Z. R.; McGilp, J. F. *J. Non-Cryst. Solids* **1992**, *147*, 148, 97.

(10) Devlin, K.; O'Kelly, B.; Tang, Z. R.; McDonagh, C.; McGilp, J. F. *J. Non-Cryst. Solids* **1992**, *135*, 8.

(11) Camostrini, R.; Carturan, G.; Ferrari, M.; Montagna, M.; Pilla, O. *J. Mater. Res.* **1992**, *7*, 745.

(12) Ferrari, M.; Camostrini, R.; Carturan, G.; Montagna, M. *Philos. Mag. B* **1992**, *65*, 251.

(13) Fan, X.; Wang, M.; Xiong, G. *Mater. Sci. Eng.* **1993**, *B21*, 55.

(14) Fan, X.; Wang, M.; Xiong, G. *J. Mater. Sci. Lett.* **1993**, *12*, 1552.

(15) Arai, K.; Namikawa, H.; Kumata, K.; Honda, T. *J. Appl. Phys.* **1986**, *59*, 3430.

(16) Arai, K.; Namikawa, H.; Ishii, Y.; Imai, H.; Hosono, H. *J. Non-Cryst. Solids* **1987**, *95*, 96, 609.

(17) Thomas, I. M.; Payne, S. A.; Wilke, G. D. *J. Non-Cryst. Solids* **1992**, *151*, 183.

(18) Fujiyama, T.; Yokoyama, T.; Hori, M.; Sasaki, M. *J. Non-Cryst. Solids* **1991**, *135*, 198.

(19) Fujiyama, T.; Hori, M.; Sasaki, M. *J. Non-Cryst. Solids* **1990**, *121*, 272.

<sup>†</sup> Department of Chemical Engineering, University of Wisconsin, Madison.

<sup>\*</sup> To whom correspondence should be addressed at the Department of Chemical Engineering and Materials Science Program (email: bray@engr.wisc.edu).

<sup>®</sup> Abstract published in *Advance ACS Abstracts*, February 15, 1995.

(1) Weber, M. J. *J. Non-Cryst. Solids* **1990**, *123*, 208.

(2) Klein, L. C. *Annu. Rev. Mater. Sci.* **1993**, *23*, 437.

(3) Brinker, C. J.; Scherer, G. W. *Sol-Gel Science*; Academic Press: Boston, 1990.

(4) Bünzli, J.-C. G.; Choppin, G. R. *Lanthanide Probes in Life, Chemical, and Earth Sciences*; Elsevier: New York, 1989.

In this paper, we demonstrate for the first time that  $\text{Eu}^{3+}$  fluorescence line narrowing (FLN) spectroscopy is a powerful tool for detecting and studying dopant ion clustering and  $\text{Al}^{3+}$  codoping effects in  $\text{Eu}^{3+}$ -doped sol-gel silica. The effects observed for  $\text{Eu}^{3+}$  are expected to impact the development of an understanding of other luminescent ion-doped sol-gel systems. The results will also assist in the identification of reaction and processing conditions conducive to the establishment of a spatially uniform distribution of luminescent ions in sol-gel materials.

FLN is based on the use of a narrow-band excitation source to selectively excite subsets of dopant ions in structurally distinct bonding sites.<sup>20,21</sup> In an amorphous host such as silica, dopant ions typically reside in a distribution of structurally inequivalent bonding sites. The site-to-site variations in local structure lead to slightly different electronic energy levels of the dopant ions. As a result, dopant ion absorption and fluorescence bands are comprised of a superposition of closely spaced contributions from ions in structurally distinct environments. This inhomogeneous broadening of the absorption and fluorescence bands is a common characteristic of ions in glasses. Because they reflect a multiplicity of bonding sites, structural interpretation of inhomogeneously broadened fluorescence bands is difficult. When a narrow-band laser source is used to excite the sample, only the subset of ions that has absorption bands resonant with the laser are excited and subsequently fluoresce. The resultant line-narrowed fluorescence spectrum is greatly simplified and more amenable to structural interpretation than the original inhomogeneously broadened spectrum.<sup>20,21</sup>

An important consideration in  $\text{Eu}^{3+}$  FLN experiments is energy transfer between adjacent  $\text{Eu}^{3+}$  ions. If there is a small spatial separation between  $\text{Eu}^{3+}$  ions, the ions resonant with the laser can transfer the excitation energy to nearby nonresonant  $\text{Eu}^{3+}$  ions with the simultaneous generation or annihilation of phonons. Energy transfer destroys site selectivity because it provides a mechanism for exciting nonresonant ions. Subsequent emission from the nonresonant ions leads to spectral broadening. In the current work, we attribute the lack of a line-narrowing effect in  $\text{Eu}^{3+}$ -doped sol-gel silica to energy transfer between neighboring  $\text{Eu}^{3+}$  ions in  $\text{Eu}^{3+}$  clusters and show that the presence of  $\text{Al}^{3+}$  as a codopant inhibits cluster formation and leads to the development of a line narrowing effect.

## Experimental Section

**Sample Preparation.** Monolithic silica gels were prepared by the acid-catalyzed hydrolysis and condensation of tetraethoxysilane (TEOS, Aldrich) with deionized water ( $10^{18}$  M $\Omega$  cm). In one set of samples, ethanol (spectrophotometric grade, Aldrich) was used as a common solvent, and the molar ratio TEOS:water:ethanol was 1:4:4 (1:4:4 samples). In another set of "alcohol-free" samples, the TEOS:water molar ratio was 1:16 (1:16 samples). Small amounts of nitric acid were added until the sol pH reached approximately 1.5.

Europium was introduced during the initial mixing stage by dissolving a hydrated europium salt ( $\text{Eu}(\text{NO}_3)_3 \cdot 6\text{H}_2\text{O}$ ,

Aldrich) in the sols described above. Salt concentrations were adjusted to give theoretical densified product compositions of  $x\text{Eu}_2\text{O}_3 - (100 - x)\text{SiO}_2$ ,  $x = 0.5-10$  wt %. These are theoretical concentrations in that they do not account for the residual hydroxyl and organic groups in the gels at various stages of the sol-gel process. Throughout this paper,  $\text{Eu}^{3+}$  concentrations are referred to as the wt %  $\text{Eu}_2\text{O}_3$  that would be present in the fully densified product.

$\text{Al}^{3+}$  codopants were introduced either by an aluminum salt or an aluminum alkoxide.  $\text{Al}^{3+}$  concentrations were varied to give  $\text{Al}^{3+}/\text{Eu}^{3+}$  molar ratios ranging from 1:1 to 10:1. In one set of samples, aluminum nitrate nonahydrate ( $\text{Al}(\text{NO}_3)_3 \cdot 9\text{H}_2\text{O}$ , Aldrich) was simply dissolved along with the europium salt in the initial sol. In a second set of samples, (di-*sec*-butoxyaluminoxy)triethoxysilane ( $(\text{BuO})_2\text{AlOSi}(\text{OEt})_3$ , Hüls Petrarch) was added to a prehydrolyzed TEOS sol. We have found that the Al-O-Si alkoxide is easier to handle and more readily forms homogeneous solutions than the commonly used aluminum *sec*-butoxide, which requires significant dilution in alcohol or water before a clear sol is obtained.<sup>22</sup> A potentially problematic feature of the Al-O-Si alkoxide was that the aluminum alkoxide end of this molecule is more reactive than the silicon alkoxide end.<sup>23</sup> To counteract this reactivity difference, our  $\text{Eu}^{3+}$ -doped, TEOS-based sols (pH = 1.5) were prehydrolyzed at room temperature for approximately 2 h prior to addition of the Al-O-Si alkoxide. The prehydrolysis provided an excess of Si-OH groups to react with the aluminum alkoxide and aluminum hydroxide groups.

The preparation method outlined by Thomas et al.<sup>17</sup> was also used in our study. This method involved adding *N,N*-dimethylformamide (Aldrich) as a drying control chemical additive. Propylene oxide was also added to the prehydrolyzed sol to help "freeze" the dopant into the silica matrix.<sup>17</sup> Details of the synthesis are found in the Thomas reference.<sup>17</sup> Note that we used europium chloride instead of neodymium chloride, and the Al-O-Si alkoxide instead of aluminum *sec*-butoxide.

For all of the above synthesis schemes, reactants were combined at room temperature in glass beakers equipped with magnetic stir bars. The alcohol-free samples initially formed two phases which became one phase after approximately 30 min of stirring, as ethanol generated by the hydrolysis reactions acted as an in situ solvent. When a single phase was formed, the samples were either sealed in plastic vials and set aside at room temperature or were sealed in glass test tubes and placed in a 40 °C bath for reaction.

A goal of sol-gel optics research is to create transparent samples with high dopant concentrations. An upper limit on the dopant concentration is established in the early stages of the sol-gel process, since high salt concentrations lead to destabilization of the sols and flocculation.<sup>3</sup> Similarly, immediate gelation of the Al-O-Si alkoxide occurs on contact with the silica sols that have high europium salt concentrations. Increasing the amount of water or alcohol allows larger amounts of salts to be dissolved. The benefits of this increased dilution, however, are largely eliminated during aging and drying, when excess salts recrystallize as the water and alcohol evaporate. For example, the maximum  $\text{Al}^{3+}/\text{Eu}^{3+}$  molar ratio that could be achieved in a transparent 5 wt %  $\text{Eu}_2\text{O}_3$  silica gel was 3, regardless of the water or alcohol concentration. As the  $\text{Eu}^{3+}$  concentration was increased, the  $\text{Al}^{3+}/\text{Eu}^{3+}$  ratio had to be lowered to obtain homogeneous, transparent samples. Of the different preparation techniques used in our study (1:4:4 vs 1:16, aluminum salt vs aluminum alkoxide), one does not appear to offer a significant advantage over the others in terms of increasing dopant concentrations.

Gel times varied from a few days to over a month depending on the water to TEOS ratio, salt concentration, solvent selection, and temperature.<sup>3,24</sup> After gelation, the samples were left sealed in their containers and were aged at 60 °C

(20) Yen, W. M. In *Optical Spectroscopy Glasses*; Zschokke, I., Ed.; D. Reidel, Publishing Co.: Dordrecht, The Netherlands, 1986; pp 23-64.

(21) Weber, M. J.; Paisner, J. A.; Sussman, S. S.; Yen, W. M.; Riseberg, L. A.; Brecher, C. J. *J. Lumin.* **1976**, *12/13*, 729.

(22) Yoldas, B. E. *Am. Ceram. Soc. Bull.* **1975**, *54*, 289.

(23) Pouxviel, J. C.; Biolot, J. P.; Dauger, A.; Huber, L. *Mater. Res. Soc. Symp. Proc.*; Materials Research Society: Pittsburgh, 1986; Vol. 73, pp 269-274.

(24) Bansal, N. P. *J. Am. Ceram. Soc.* **1990**, *73*, 2647.

for 2 days in a box furnace. The seal on the top of the vials was broken after two days and the furnace was slowly (5 °C/h) ramped to 90 °C. The slow heating was performed in an effort to produce crack-free samples.

Thermal densification of the aged gels was performed in quartz crucibles in air. The furnace temperature was ramped at 1 °C/min to 200, 400, and 600 °C, with 24 h dwell times at each temperature. Samples were then heated to 800 and 900 °C for 12 h at each temperature. At 200 °C, the samples had a yellow-brown color which is attributed to decomposition products of the organics and salt counterions.<sup>6</sup> The 1:4:4 samples, which contain excess ethanol, gave a stronger color than their 1:16 counterparts. Nitrate salts in particular led to a strong yellow color at these temperatures, and the intensity of the color increased with nitrate concentration. The observable colors were largely eliminated once the samples are heated to temperatures greater than 400 °C.<sup>6</sup> Samples heated between 400 and 800 °C were generally clear and transparent.

As expected, cracking was a problem in many of the samples. All of the 1:4:4 samples cracked significantly during aging and drying. The 1:16 samples were less likely to crack, and several samples remained crack-free with slow heating to 800 °C. The Thomas approach<sup>17</sup> led to crack-free cylindrical monoliths. The presence of large dopant concentrations increased the propensity toward cracking during drying.

An important conclusion of this sample preparation study is that although characteristics such as gel times and propensity toward cracking were different for the different preparation methods, the spectroscopy of the Eu<sup>3+</sup> ions in these samples were all very similar for samples of the same product composition. This was particularly true for the samples densified at temperatures  $\geq 400$  °C. For example, we have observed no aluminum precursor-dependent effects on the spectral properties of Eu<sup>3+</sup> in densified silica gels co-doped with Al<sup>3+</sup>.<sup>7,8</sup> These results suggest that while different processing conditions lead to different microstructural properties (density, pore size, etc.), the bonding environment of Eu<sup>3+</sup> ions is not affected by the synthesis scheme once the materials are heated to temperatures greater than 400 °C.

**Spectroscopic Measurements.** Continuous-wave, broad-band fluorescence spectra were obtained by exciting samples with the 514.5 nm line of a Coherent Innova Series 70-5 argon ion laser or a tungsten lamp equipped with a dielectric filter passing all wavelengths less than 500 nm. Fluorescence was focused on the entrance slit of a SPEX 1000M 1-m monochromator. The detector was a multialkali photomultiplier tube (PMT) connected to photon-counting electronics (SPEX).

Time-resolved fluorescence line narrowing experiments were carried out using a pulsed laser system comprised of a Q-switched Nd:YAG laser (Continuum NY-61) and a pulsed dye laser (Spectra-Physics PDL-3). The dye was a 60:40 mixture of rhodamine 590 and rhodamine 610 which provided the tunable laser light from 570 to 585 nm used to excite the  ${}^7F_0 \rightarrow {}^5D_0$  transition of Eu<sup>3+</sup>. Fluorescence was focused on a SPEX 1704 1-meter monochromator. The detector consisted of a Hamamatsu R2228 PMT. The PMT was connected to photon-counting electronics consisting of a fast preamplifier (ORTEC 9301), an amplifier discriminator (ORTEC 9302), and photon counter (ORTEC 994). The PMT could also be connected to a Stanford Research Systems boxcar integrator which allowed variable control of a sampling gate of user-set width and delay. Luminescence decay scans were recorded using a LeCroy ScopeStation 140 digital oscilloscope. The signal from the PMT was typically terminated into a 1 k $\Omega$  resistor, giving an instrument response time constant of approximately 0.5  $\mu$ s. A photodiode was used to generate the electronic pulse used to trigger and synchronize the electronics.

Fourier transform infrared (FTIR) measurements were performed on a Mattson Galaxy 5020 spectrometer equipped with a CsI beam splitter and DTGS detector. Samples were prepared with the standard KBr pellet method.

## Results and Discussion

**Eu<sup>3+</sup> Clustering in Doped Silica Gels.** Clustering or aggregation of dopant ions is a significant issue in

the synthesis of sol-gel optics, since clustering generally leads to adverse effects such as concentration quenching.<sup>17</sup> When severe, dopant ion clustering can be identified by techniques such as X-ray diffraction XRD<sup>25</sup> or TEM.<sup>26</sup> Fluorescence decay (lifetime) measurements have also been used to identify clustering in Nd<sup>3+</sup>-doped systems.<sup>15-19</sup> The energy level structure of Nd<sup>3+</sup> provides an efficient cross-relaxation mechanism which leads to nonradiative decay and short fluorescence lifetimes when Nd<sup>3+</sup> ions are spatially close in the material. A disadvantage of using lifetime measurements to identify clustering is the fact that lifetimes are also affected by hydroxyl groups in the sol-gel silica matrix, which also lead to non-radiative decay and shorter lifetimes.<sup>27</sup>

Clustering in Eu<sup>3+</sup>-doped silica gels is less well-established than Nd<sup>3+</sup> clustering. The Eu<sup>3+</sup> energy level structure does not provide the efficient cross relaxation pathway found in Nd<sup>3+</sup>, so concentration quenching is less significant. For example, we have found that the lifetimes remain approximately constant and the fluorescence signal increases as the Eu<sup>3+</sup> concentration is increased from 1 to 10 wt % in similarly prepared samples. Fan et al.<sup>13</sup> have studied concentration effects in Eu<sup>3+</sup>-doped sol-gel silica and did not observe concentration quenching in gel glass with concentrations as high as 20 wt % (4 mol %). These observations, however, do not necessarily lead to the conclusion that Eu<sup>3+</sup> ions are well-isolated in the silica matrix.

Eu<sup>3+</sup> fluorescence line narrowing studies provide an alternative method for identifying clustered rare-earth ions. Figure 1 presents the broadband fluorescence and FLN spectra for a 1 wt % Eu<sub>2</sub>O<sub>3</sub> silica gel densified at 800 °C. The broad-band spectrum is qualitatively similar to what is observed in melt-derived silicate systems,<sup>5</sup> which has led to the conclusion that the Eu<sup>3+</sup> bonding environment in sol-gel and melt-derived systems are structurally similar. Note, however, in contrast to melt-derived glasses,<sup>20</sup> the sol-gel system shows a lack of any significant line narrowing. This lack of a line-narrowing effect was observed for all Eu<sup>3+</sup> concentrations encountered in our study (0.5–10 wt % Eu<sub>2</sub>O<sub>3</sub>). The lack of line narrowing was also observed by Camprostrini et al.<sup>11</sup>

We attribute the lack of line narrowing to phonon-assisted energy transfer between adjacent Eu<sup>3+</sup> ions in Eu<sup>3+</sup> clusters. During the FLN experiment, only the subset of Eu<sup>3+</sup> ions with a  ${}^7F_0 \rightarrow {}^5D_0$  band resonant with the laser are directly excited. Because of the proximity of the ions in the clusters, however, those ions resonant with the laser can transfer their energy to nonresonant Eu<sup>3+</sup> ions with the simultaneous creation or annihilation of phonons. The phonon-assisted energy-transfer process populates an ensemble of Eu<sup>3+</sup> ions, destroying the site selectivity of the experiment. The resultant emission is consequently broadened. In addition, we cite the appearance of nonresonant  ${}^5D_0 \rightarrow {}^7F_0$  emission centered near 578 nm as particularly strong evidence of energy transfer. This peak is identified with an asterisk in Figure 1.

(25) Tanaka, K.; Kamiya, K. *J. Mater. Sci. Lett.* **1991**, *10*, 1095.

(26) Moreshead, W. V.; Nogues, J. R.; Krabill, R. H. *J. Non-Cryst. Solids* **1990**, *121*, 267.

(27) Horrocks, W. DeW., Jr.; Sudnick, D. R. *J. Am. Chem. Soc.* **1979**, *101*, 334.

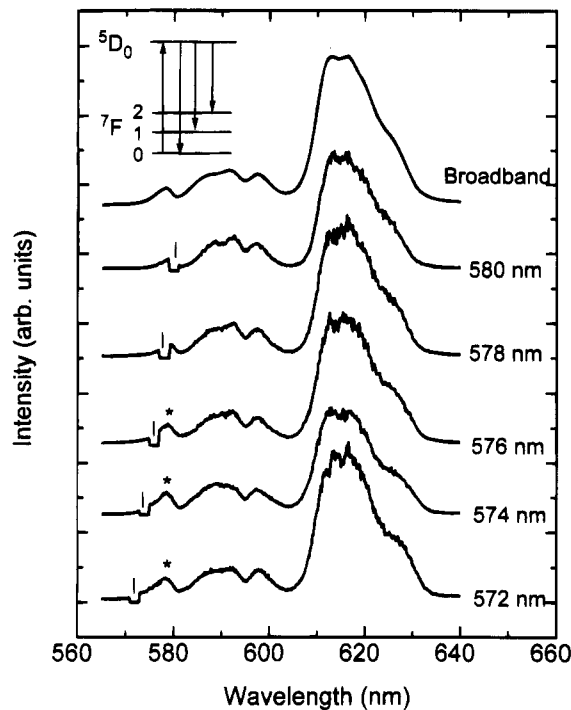


**Figure 1.** Fluorescence line-narrowed spectra (77 K) of 1 wt %  $\text{Eu}_2\text{O}_3$ -doped silica gel densified in air at 800 °C. Spectra collected in photon-counting mode. Dye laser excitation wavelengths are listed and are indicated by vertical lines. The broad-band spectrum was excited by a tungsten lamp passing all wavelengths  $\leq 500$  nm. Spectra are normalized to the  $^5\text{D}_0 \rightarrow ^7\text{F}_1$  peak intensity. Nonresonant  $^5\text{D}_0 \rightarrow ^7\text{F}_0$  emission is indicated with an asterisk (see text).

Clustering of  $\text{Eu}^{3+}$  ions in the silica matrix is not unexpected. Previous work by our group has shown that a significant fraction of the  $\text{Eu}^{3+}$  ions do not show a strong interaction with the silica matrix, even after gelation of these samples.<sup>6</sup> Because these ions have only weak interactions with the silica matrix during the early stages of the densification process, they can aggregate and form clusters as pore liquid evaporates. Thomas et al. added propylene oxide to their silica sol in an effort to combat dopant ion mobility and to effectively “freeze” the dopant ions in the silica matrix during gelation.<sup>17</sup> We note, however, that we observed a lack of line-narrowing in  $\text{Eu}^{3+}$ -doped silica gels prepared by the Thomas technique. This suggests that the propylene oxide was not completely effective in stabilizing the dopant ions in the silica gel. This is consistent with the fact that the Thomas group was unable to achieve lasing in their  $\text{Nd}_2\text{O}_3\text{-SiO}_2$  systems, likely a result of  $\text{Nd}^{3+}$  clustering. It was not until the material was codoped with  $\text{Al}^{3+}$  that lasing was demonstrated ( $\text{Al}^{3+}$  codoping effects are discussed in the next section).

We have attempted to use time-resolved fluorescence line narrowing to observe the temporal evolution of the spectra during the  $\text{Eu}^{3+}\text{-Eu}^{3+}$  energy transfer. Figure 2 presents FLN spectra collected at fixed gate delays after excitation by a 574 nm laser pulse. No significant line-narrowing is observed, even at gate delays as short as 5  $\mu\text{s}$ . We again note the appearance of nonresonant  $^5\text{D}_0 \rightarrow ^7\text{F}_0$  emission near 578 nm as direct evidence of energy transfer. These results suggest that the  $\text{Eu}^{3+}\text{-Eu}^{3+}$  energy transfer is very efficient, occurring on a

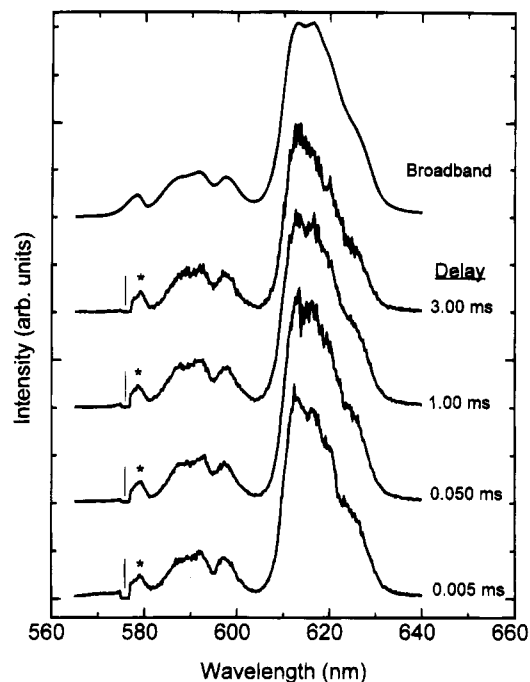


**Figure 2.** Time-resolved fluorescence line-narrowed spectra (77 K) of 1 wt %  $\text{Eu}_2\text{O}_3$ -doped silica gel densified in air at 800 °C. Pulsed dye laser excitation wavelength: 574 nm. Sampling gate delays are listed. The broad-band spectrum was excited by a tungsten lamp passing all wavelengths  $\leq 500$  nm. Spectra are normalized to the  $^5\text{D}_0 \rightarrow ^7\text{F}_1$  peak intensity. Nonresonant  $^5\text{D}_0 \rightarrow ^7\text{F}_0$  emission is indicated with an asterisk (see text).

time scale faster than what is currently accessible in our experiment.

This fast energy-transfer process is explainable in terms of previous energy transfer studies, where efficient  $\text{Eu}^{3+}\text{-Eu}^{3+}$  energy transfer has been identified.<sup>28</sup> We expect the  $\text{Eu}^{3+}\text{-Eu}^{3+}$  spatial separation in the clusters to be similar to that found in  $\text{Eu}_2\text{O}_3$  (approximately 3.6 Å).<sup>24</sup> In a study of  $\text{Eu}^{3+}\text{-Eu}^{3+}$  energy transfer in europium oxide, Buijs et al.<sup>28</sup> calculated an energy-transfer probability of approximately  $2 \times 10^6 \text{ s}^{-1}$ . This places the time scale of the  $\text{Eu}^{3+}\text{-Eu}^{3+}$  energy transfer in the submicrosecond range, which is consistent with the time-resolved FLN data presented in Figure 2.

Given this interpretation, FLN studies can be used to identify clustered  $\text{Eu}^{3+}$  ions in a variety of sol-gel systems. Our results show that in the absence of codopants, rare-earth-ion clustering is significant in sol-gel silica, even at low dopant concentrations and despite the transparency of the samples, local inhomogeneities are likely to exist.

**$\text{Al}^{3+}$  Codoping Effects. Broad-Band Fluorescence.** Figure 3 presents fluorescence spectra for 1 wt %  $\text{Eu}_2\text{O}_3$  silica gels containing  $\text{Al}^{3+}$  densified at 800 °C. The  $\text{Al}^{3+}/\text{Eu}^{3+}$  molar ratio is indicated with each spectrum. As seen in Figure 3,  $\text{Al}^{3+}$  codoping significantly affects the  $\text{Eu}^{3+}$  fluorescence spectrum. The fact that small amounts of  $\text{Al}^{3+}$  lead to significant changes in the  $\text{Eu}^{3+}$  spectra indicates that the  $\text{Eu}^{3+}$  ions preferentially interact with  $\text{Al}^{3+}$  groups. As the  $\text{Al}^{3+}/\text{Eu}^{3+}$  molar ratio is increased, the changes in the spectra become more pronounced.

(28) Buijs, M.; Meyerink, A.; Blasse, G. *J. Lumin.* **1987**, *37*, 9.

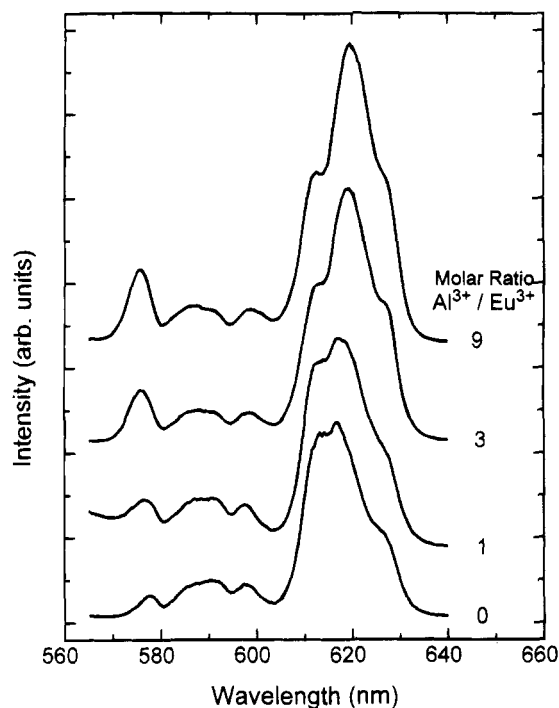


**Figure 3.** Room-temperature fluorescence spectra of codoped silica gels with various  $\text{Al}^{3+}/\text{Eu}^{3+}$  molar ratios.  $\text{Al}^{3+}$  introduced by aluminum nitrate. Tungsten lamp excitation passing all wavelengths  $\leq 500$  nm. All samples contain 1 wt %  $\text{Eu}_2\text{O}_3$  and were densified at 800 °C.  $\text{Al}^{3+}/\text{Eu}^{3+}$  molar ratios are indicated with each spectrum. Spectra are normalized to the  ${}^5\text{D}_0 \rightarrow {}^7\text{F}_1$  peak intensity.

Relative to the spectrum of the sample containing no  $\text{Al}^{3+}$ , four major changes associated with the interaction between  $\text{Eu}^{3+}$  and  $\text{Al}^{3+}$  groups are observed. First, codoping with  $\text{Al}^{3+}$  leads to increased relative intensity of the  ${}^5\text{D}_0 \rightarrow {}^7\text{F}_0$  fluorescence band ( $\sim 570$ – $580$  nm). Second, the peak of the  ${}^5\text{D}_0 \rightarrow {}^7\text{F}_0$  band shifts to higher energy (shorter wavelength). Third, the  ${}^5\text{D}_0 \rightarrow {}^7\text{F}_2$  fluorescence band ( $\sim 610$ – $630$  nm) increases in relative intensity, with the increased intensity appearing on the low-energy side of this band. Fourth, all fluorescence bands show increased inhomogeneous broadening. In the present study, we use these observations as qualitative indicators of  $\text{Eu}^{3+}$ – $\text{Al}^{3+}$  interactions in the materials. A more detailed, structure and bonding analysis based on site symmetry, crystal field analysis, and covalency/ionicity arguments is being pursued and will be presented in a future paper.

**Fluorescence Line-Narrowing Studies.** Figure 4 shows a typical set of FLN spectra for  $\text{Eu}^{3+}$ -doped silica gels codoped with  $\text{Al}^{3+}$ . Unlike the samples with no  $\text{Al}^{3+}$  (Figures 1 and 2), these spectra show dramatic line-narrowing effects, with line-narrowed fluorescence peaks shifting and changing relative intensity as the excitation wavelength is varied. The energy-transfer problems associated with clustered  $\text{Eu}^{3+}$  ions have largely been eliminated, which indicates that  $\text{Al}^{3+}$  codoping is indeed effective in isolating  $\text{Eu}^{3+}$  in the silica matrix.

Regarding the preparation technique, we note that both methods of  $\text{Al}^{3+}$  incorporation, salt and alkoxide, were equally effective at dispersing  $\text{Eu}^{3+}$  ions in the silica matrix.<sup>7,8</sup> Fujiyama et al.<sup>18</sup> have suggested that a rare earth–aluminum double metal alkoxide structure was required to successfully disperse  $\text{Nd}^{3+}$  ions in a silica matrix. While their method may be more effective

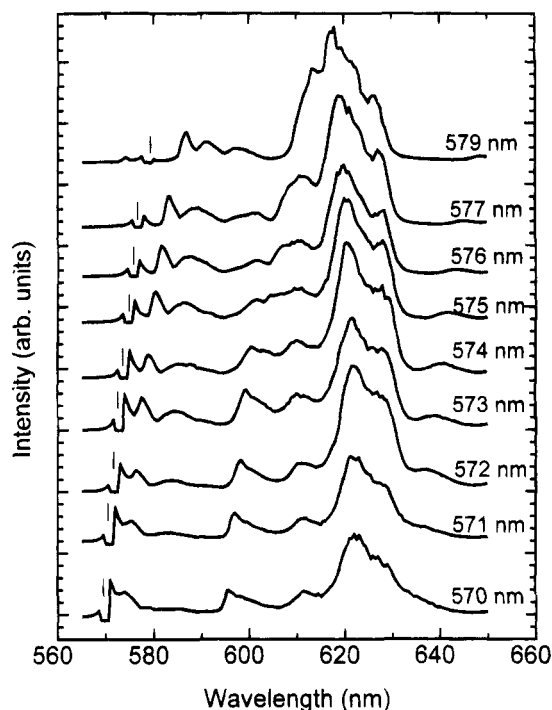


**Figure 4.** Fluorescence line-narrowed spectra (77 K) of codoped silica gel densified in air at 800 °C (1 wt %  $\text{Eu}_2\text{O}_3$ ,  $\text{Al}^{3+}/\text{Eu}^{3+}$  molar ratio = 10).  $\text{Al}^{3+}$  introduced by aluminum nitrate. Spectra collected in photon-counting mode. Dye laser excitation wavelengths are listed and are indicated by vertical lines. Spectra are normalized to the  ${}^5\text{D}_0 \rightarrow {}^7\text{F}_1$  peak intensity.

for high rare-earth concentrations, in the concentration range encountered in our study, the simple aluminum salt method has been demonstrated to be equally effective.

Tuning the dye laser to different regions of the absorption band allows selective excitation of  $\text{Eu}^{3+}$  ions in different types of sites. For example, Figure 3 showed that  $\text{Al}^{3+}$  codoping led to shorter wavelength  ${}^5\text{D}_0 \rightarrow {}^7\text{F}_0$  emission (peak  $\sim 575$  nm) and longer wavelength  ${}^5\text{D}_0 \rightarrow {}^7\text{F}_2$  emission ( $\sim 620$ – $630$  nm). By tuning the dye laser to wavelengths  $< 575$  nm, we can preferentially excite those  $\text{Eu}^{3+}$  ions that are interacting with the  $\text{Al}^{3+}$  groups. Alternatively, long-wavelength  ${}^7\text{F}_0 \rightarrow {}^5\text{D}_0$  excitation ( $\geq 579$  nm) yields fluorescence spectra suggestive of clustered  $\text{Eu}^{3+}$  ions. This illustrates the utility of the FLN technique in deconvoluting the spectra of isolated and clustered rare-earth ions in these materials.

**Fluorescence Decay Studies.** Fluorescence decay measurements provide additional information on the bonding environment of  $\text{Eu}^{3+}$  ions in sol–gel silica. In particular, the decay is sensitive to the presence of hydroxyl groups in the  $\text{Eu}^{3+}$  coordination sphere.<sup>27</sup>

Representative results are presented in Table 1. Decay times measured in this study show slight deviations from exponentiality, which is attributed to accidental degeneracy. For the sake of comparison, we have fit each decay curve with a single exponential, the time constant of which is reported as the lifetime of the decay in Table 1.

The most apparent finding of the decay studies is that when  $\text{Al}^{3+}$  is introduced into the silica matrix, the  $\text{Eu}^{3+}$  decay times are shorter than in samples with no  $\text{Al}^{3+}$ . This effect is explained in terms of hydroxylation. Previous work has shown that alumina gels have several hydroxylated phases depending on the treat-

**Table 1. 1 wt % Eu<sup>3+</sup> Silica Gels Densified at 900 °C Al<sup>3+</sup> Introduced via Aluminum Nitrate (Lifetimes Measured at Room Temperature)**

molar ratio Al/Eu	excitation wavelength (nm)	emission wavelength (nm)	exponential lifetime (ms ± 0.05 ms)
0	578	612	1.81
1	575	630	0.92
	575	620	0.97
3	575	610	1.25
	573	630	0.87
	575	620	0.88
9	578	610	0.97
	573	630	0.89
	575	620	0.92
	578	610	1.08

ment temperature.<sup>3</sup> In Al<sup>3+</sup>-doped silica gels, it is likely that the Al<sup>3+</sup> groups remain significantly hydroxylated. Since we have demonstrated that Eu<sup>3+</sup> preferentially interacts with Al<sup>3+</sup> groups, Eu<sup>3+</sup> ions are more likely to interact with hydroxyl groups in Al<sup>3+</sup>-containing samples. This raises the possibility that while Al<sup>3+</sup> codoping has the beneficial effect of increasing Eu<sup>3+</sup> dispersion and isolation, it may have the adverse effect of increasing the hydroxyl concentration in the vicinity of the Eu<sup>3+</sup> ions.

We have attempted to quantify the hydroxyl content of samples with and without Al<sup>3+</sup> codopants using FTIR spectroscopy. These results, however, were largely inconclusive, most likely due to the fact that the Al<sup>3+</sup> concentration is low in these samples. In all cases, the IR spectra were dominated by that of the silica matrix.

Site-selective lifetime measurements reinforce the conclusion that Eu<sup>3+</sup> ions interacting with Al<sup>3+</sup> groups are more hydroxylated. We showed in Figures 3 and 4 that Al<sup>3+</sup> codoping leads to a short wavelength <sup>5</sup>D<sub>0</sub> ↔ <sup>7</sup>F<sub>0</sub> band and a long-wavelength <sup>5</sup>D<sub>0</sub> → <sup>7</sup>F<sub>2</sub> emission band. We can selectively excite regions of the <sup>7</sup>F<sub>0</sub> →

<sup>5</sup>D<sub>0</sub> band and selectively detect regions of the <sup>5</sup>D<sub>0</sub> → <sup>7</sup>F<sub>2</sub> band, which allows a degree of site specificity in our fluorescence decay measurements. When we selectively measure the fluorescence decay of Eu<sup>3+</sup> ions interacting with Al<sup>3+</sup> groups (short wavelength <sup>7</sup>F<sub>0</sub> → <sup>5</sup>D<sub>0</sub> excitation, long wavelength <sup>5</sup>D<sub>0</sub> → <sup>7</sup>F<sub>2</sub> emission), we observe the shortest lifetimes for a given sample. Alternatively, the longest lifetimes are observed when we selectively excite and detect clustered Eu<sup>3+</sup> ions (long-wavelength <sup>7</sup>F<sub>0</sub> → <sup>5</sup>D<sub>0</sub> excitation and short-wavelength <sup>5</sup>D<sub>0</sub> → <sup>7</sup>F<sub>2</sub> emission).

### Conclusion

We have developed an interpretation of Eu<sup>3+</sup> fluorescence line-narrowing spectra that allows identification of clustered and isolated rare-earth ions in sol-gel silica. We have shown that in the absence of codopants such as Al<sup>3+</sup>, rare-earth-ion clustering may be more significant than previously reported. Even in transparent monoliths with Eu<sup>3+</sup> concentrations <1 wt %, significant ion clustering occurs. Al<sup>3+</sup> codoping inhibited clustering and provided a more uniform distribution of Eu<sup>3+</sup> in the matrix, as Eu<sup>3+</sup> preferentially interacts with Al<sup>3+</sup> groups. Fluorescence decay measurements suggest that Al<sup>3+</sup> codoping may increase the hydroxyl concentration in the vicinity of Eu<sup>3+</sup> ions.

**Acknowledgment.** The authors are grateful to Benson Chandra and Tedy Lim for their assistance in sample preparation and for Bryan Pivovar's assistance in the FTIR measurements. We acknowledge partial financial support from the National Science Foundation and the University of Wisconsin Graduate School. M.J.L. acknowledges fellowship support from the Amoco Corp.

CM940481J